Polymer Journal, Vol. 14, No. 12, pp 985—992 (1982)

Structure and Mechanical Properties of Sequential Interpenetrating Polymer Networks II. Complex-Forming Polyoxyethylene: Poly(acrylic acid) Systems[1]

Hiroshi ADACHI,* Shiro NISHI, and Tadao KOTAKA**

Department of Macromolecular Science, Faculty of Science, Osaka University, Toyonaka, Osaka 560, Japan

(Received July 17, 1982)

ABSTRACT: Two types of interpenetrating polymer networks (IPNs) consisting of complex-forming polyoxyethylene (POE) and poly(acrylic acid) (PAA) as the first and second components, respectively, were prepared by matrix polymerization. One type of IPNs was semi-IPNs in which only PAA was crosslinked, and the other was full-IPNs with both POE and PAA crosslinking. Differential scanning calorimetry and solvent extraction on the semi-IPNs showed that POE forms a 1 : 1 complex with PAA and that only excess POE can be extracted. This complex formation may apply to the full-IPNs in which POE is not in excess of PAA. The glass transition temperature T_g, dynamic and static mechanical properties, and stress-strain behavior were examined. The semi- and full-IPNs with the PAA content between 30 and 60 mol% appeared to be single-phase systems, in which either amorphous POE or PAA was mixed with POE : PAA (1 : 1) complexes. These IPNs exhibited only one fairly sharp glass transition. In IPNs with either low or high PAA content, semicrystalline POE or amorphous PAA microdomains, respectively, were phase-separated from the complex phase. The extent of microphase separation was less in the full-IPNs than in the corresponding semi-IPNs.

KEY WORDS Polymer Complex / Interpenetrating Polymer Networks / Complex-Forming IPN / Polyoxyethylene / Poly(acrylic acid) / Glass Transition / Viscoelastic Properties / Stress-Strain Curves / Failure Envelope /

Interpenetrating polymer networks (IPNs) are a special type of polymer blends designed to obtain compatible materials irrespective of the mutual miscibility-immiscibility of the constituent polymers.[3-6] One of the most common IPNs is the so-called sequential IPNs (SIPNs). In preparing an SIPN of polymer (I) and polymer (II), a preformed network of polymer (I) is swollen with a monomer (II) containing a crosslinker and an initiator, and the monomer (II) is polymerized and crosslinked *in situ*.[2-6] We examined SIPNs consisting of a pair of semicompatible poly(ethyl acrylate) (PEA) and poly(methyl methacrylate) (PMMA) as the (I) and (II) components, respectively.[7,8] We concluded that in the preformed PEA network, the MMA mixture first yields microgels which eventually interconnect to form an SIPN having two mutually interpenetrating continuous phases. Such an IPN usually has a broad relaxation region covering the glass transition regions of the two constituent polymers.[8]

Interpolymer complexes are another special type of polymer blends formed by specific interactions of the constituent polymers.[9,10] Such interactions may be coulombic attraction in polyelectrolyte complexes,[11] hydrogen bondings in polyether : poly(carboxylic acid) complexes,[12,13] or van der Waals interactions in certain stereocomplexes.[14] Because of these specific interactions, an interpolymer complex often gives a molecularly-mixed blend but only with a certain stoichiometric composition. For example, the mixing of aqueous solutions of polyoxy-

* Present address: *Manufacturing Development Laboratory, Mitsubishi Electric Corporation, Amagasaki, Hyogo 661, Japan.*

** To whom correspondence should be addressed.

ethylene (POE) and poly(acrylic acid) (PAA) leads to an equimolar POE : PAA complex containing hydrogen bonds.[12] If acrylic acid (AA) monomers are polymerized in the presence of POE, the polymerization with the POE molecules as a template proceeds to form an equimolar POE : PAA complex.[12] Such a POE : PAA complex can be reversibly dissociated and reformed by adjusting the pH of the system.[12,13] Therefore, if we can engineer such a polymer complex into a membrane with sufficient strength, we should be able to obtain a *chemical valve*,[15] which can be operated by adjusting the chemical environment of the system. Obviously, the POE : PAA complex alone cannot be a *chemical valve*, since the membrane disengages upon complex dissociation. One apparent way to avoid this difficulty may be to prepare an SIPN membrane composed of the interpolymer complex. Consequently, we undertook a study on the preparation, characterization and survey of the physical properties of complex-forming POE : PAA SIPNs[16] and the results are presented in this paper. An attempt was made to utilize this membrane as a mechanochemical system or a chemical valve, as will be described elsewhere.

EXPERIMENTAL

Materials Hydroxyl terminated polyoxyethylene (POE) was a commercial material purchased from Nakarai Chemicals, Ltd. Its catalogue molecular weight was 7800—9000. The POE was purified by twice precipitating it in excess *n*-hexane from a hot toluene solution and dried *in vacuo* at 50°C. Acrylic acid (AA) monomer and divinylbenzene (DVB) were distilled under reduced nitrogen atmosphere just before use. Trimethylolpropane was purified by sublimating it under reduced pressure at 60°C. All other chemicals were of reagent grade and used without further purification.

Semi-IPNs consisting of uncrosslinked POE and crosslinked PAA were prepared as follows: A prescribed amount of POE was dissolved in AA monomer containing 1 mol% DVB and 1 wt% benzoylperoxide (BPO). The mixture was main-

Table I. Characteristics of POE : PAA IPN specimens[a,b]

Code	PAA / wt%	PAA / mol%	Sol fraction[c] / wt%	T_g[d] / K	Degree of crystallinity[d] χ_c / wt%
Semi-IPNs (S-series)					
POE[a]	0.0	0.0	100	224	93.7
S-17	25.0	16.9	60.9	235	54.5 (72.7)[e]
S-33	44.8	33.2	35.4	249	—
S-42	54.4	42.2	19.4	264	—
S-50	62.1	50.0	3.6	277	—
S-58	68.9	57.5	4.4	320	—
S-66	75.7	65.6	2.4	344	—
Full-INPs (F-series)					
cr-POE[f]	0.0	0.0	16.6	213	51.1
F-15	22.5	15.1	11.6	233	28.9 (37.3)[e]
F-31	41.8	30.5	6.3	244	—
F-48	59.7	47.5	5.0	272	—
F-65	74.6	64.5	7.5	337	—

[a] POE prepolymer with hydroxyl terminals (MW = 7800—9000).
[b] AA mixture containing POE prepolymer with 1 mol% DVB and 1 wt% BPO was polymerized at 80°C for 48 h.
[c] Extracted with methanol for 5 h.
[d] From DSC.
[e] Degree of crystallinity in POE portion by wt% of total film and (of POE).
[f] POE crosslinked with 17 mol% TMP, 50 mol% MDI, and 0.05 wt% di-*n*-butyltin dilaurate at 80°C for 24 h.

tained at 80°C for 48 h in a sealed polymerization cell. The specimen obtained was then quenched and dried *in vacuo* at room temperature for 7 days to remove unreacted monomers. The weight loss during the drying process was within a few percent, indicating that the conversion was nearly 100%. The semi-IPN specimens were coded the S-series.

In preparing the full-IPNs coded F-series, the POE was first chain-extended and crosslinked at terminal hydroxyl groups. The POE prepolymer was mixed with 17 mol% trimethylolpropane (TMP), 50 mol% 4,4′-diphenylmethane diisocyanate (MDI), and 0.05 mol% di-*n*-butyltin dilaurate as the catalyst. The mixture was left standing at 80°C for 48 h in the polymerization cell. Then, the crosslinked POE film (cr-POE) obtained was swollen to a specified extent with the same AA/DVB/BPO mixture used for the semi-IPN preparation. The swollen film was again maintained at 80°C for 48 h in the cell. Unreacted monomers were removed by the same drying procedure mentioned above. The characteristics of the semi- and full-IPNs are summarized in Table I.

Methods For determining the sol fraction, or more precisely, the fraction extractable from as-synthesized IPN samples, each sample was extracted by methanol refluxing for 5 h. The specimen was dried *in vacuo* until constant weight within 0.1% was attained.

Thermal analyses were made with a differential scanning calorimeter (DSC; Rigakudenki model 8055) over a temperature range from 173 to 420 K with a heating rate of about 10 K min^{-1} under nitrogen atmosphere. Dynamic mechanical measurements were made with a Rheovibron DDV-II (Toyo-Baldwin Co.) at 110 Hz over a temperature range from 130 to 450 K with a heating rate of about 1 K min^{-1} under dry nitrogen stream.

Static mechanical measurements were carried out with a tensile tester (Iwamoto Seisakusho, Kyoto) at temperatures regulated to within ± 0.5 K under dry air. Tensile stress-strain curves were obtained in a range of strain rate $\dot{\varepsilon}$ from 0.6 to 80% s^{-1} or in a temperature range from 286 to 353 K with a constant $\dot{\varepsilon}$ of 5.3% s^{-1}. Tensile stress relaxation tests were made over a temperature range from 290 to 320 K. At low temperatures the strain ε was 0.02, and at high temperatures, 0.04. The initial strain rate was about 390% s^{-1}. Tensile creep tests were carried out in a stress range from 0.2 to 10.0 MPa at 303 K. The stress was regulated to within $\pm 2\%$. The creep was observed for 6000 s.

RESULTS AND DISCUSSION

Structure of the IPNs

Figure 1 shows the DSC thermograms of as-synthesized, unextracted semi- and full-IPNs, POE, and cr-POE samples. The thermograms of all these samples exhibit only one glass transition. Endothermic peaks due to the melting of POE crystallites can be seen only in the thermograms of the four samples: at 322 K for POE and at 311 K for cr-POE and at temperatures somewhat lower than these temperatures for semi-IPN S-17 and full-IPN F-15 both with relatively low PAA content. From the areas under the endothermic peaks, the degrees

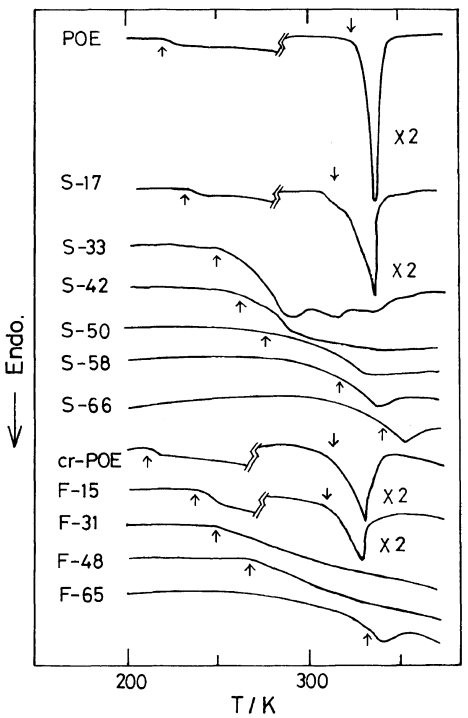

Figure 1. DSC thermograms of semi (S)- and full (F)-IPNs with a heating rate of 10 K min^{-1} under nitrogen atmosphere. For comparison, the thermograms of uncrosslinked POE and crosslinked POE are also shown. The endothermic peaks due to POE melting are shown in the half scale. Arrows (↑) denote glass transition temperatures and (↓) melting temperatures.

of crystallinity χ_c in the POE phase were estimated by employing 185 J g^{-1} for the specific enthalpy of POE crystalline melting.[17] In Table I, the χ_c for cr-POE is lower than that for POE, and similarly, the χ_c for F-15 is much lower than that for cr-POE. The interpenetration and, probably, the complex formation between the two components reduce the χ_c of the POE phase in the IPN samples.

Figure 2 shows plots of the melting temperature T_m and the glass transition temperature T_g (determined by DSC) against the PAA content (in wt%). Both S-17 and F-15 exhibit melting point depression, because their amorphous POE phase contains PAA, which is probably in the form of a POE : PAA complex. It should be noted that the T_g's of both semi- and full-IPNs fall on the same curve. The T_g increases slowly up to the equimolar composition, and then increases rapidly with increasing PAA content. Figure 2 also shows the brittle temperature T_b (where stress-strain curves show a transition from brittle to plastic behavior) determined by Smith *et al.*[13] on a POE : PAA

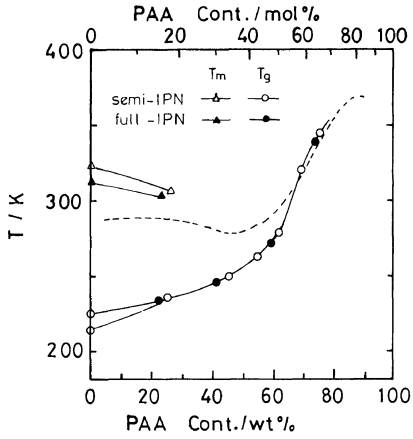

Figure 2. Plots of glass transition temperature T_g and melting temperature T_m *versus* PAA content in wt% for POE, cr-POE and semi- and full-IPNs.

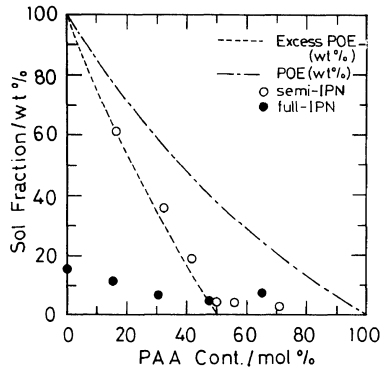

Figure 3. Plots of extractable sol fraction *versus* PAA content in mol% for semi- and full-IPNs subjected to boiling point extraction with methanol for 5 h. The dot-dash line represents POE content in wt% of the IPNs. The broken line represents the amount of excess POE over crosslinked PAA.

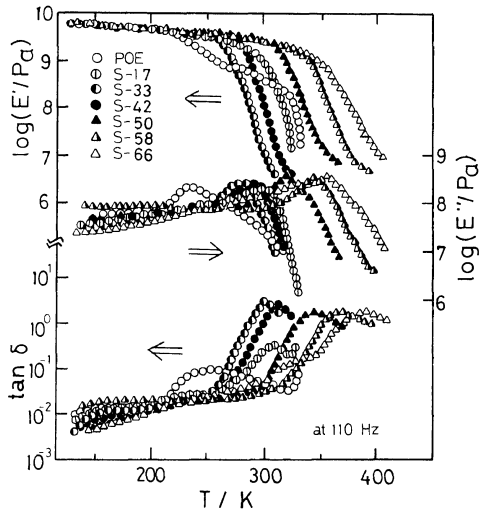

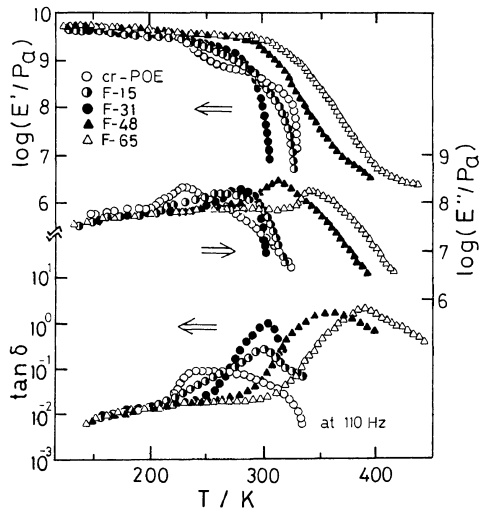

Figure 4. Plots of tensile storage E' and loss E'' moduli and loss tangent δ *versus* temperature for (a) POE and semi-IPNs and for (b) crosslinked POE and full IPNs obtained at 110 Hz.

complex and blends. In the region of high PAA content, the T_b data for blends roughly coincide with the T_g data for IPNs. However, in the region of low PAA content, the T_b is almost independent of PAA content and much higher than the T_g determined by DSC. Probably, the presence of POE crystallites in these samples obscures the brittle temperature. Similar behavior was found in the mechanical loss maximum temperature T_{max} for our semi- and full-IPNs, as will be shown below (*cf.*, Figures 4a and 4b).

Kinetic studies on the polymerization of AA in the presence of POE[12] revealed that growing PAA chains associate with preexisting POE chains until the amount of PAA exceeds that of the POE. The product is an interpolymer complex of so-called ladder-like structure, in which each oxyethylene residue forms a complex with an AA residue through hydrogen bonding. In the synthesis of POE : PAA SIPNs, similar template polymerization is likely to take leading to the formation of an IPN with the ladder-like complex. To confirm this, we examined extractable fractions of the semi- and full-IPNs. Figure 3 shows the extractable fraction in wt% plotted against the PAA content in mol% of the IPNs. In this figure, the dash-dot line represents the POE content in wt%, while the broken line represents the amount of POE present in excess of PAA. All the data points for the semi-IPNs fall on the broken line, suggesting that in the semi-IPNs, only the excess POE is extractable and the unextractable POE forms a ladder-type 1 : 1 complex with PAA rather than a nonstoichiometric complex of a so-called scrambled-salt structure.[11] It is likely that the similar 1 : 1 complex is formed in the full-IPNs, although the excess POE cannot be extracted owing to the pre-existing crosslinks.

Dynamic Mechanical Properties

Figures 4a and 4b show plots of tensile storage E' and loss E'' moduli and loss tangent δ *versus* temperature for POE and semi-IPNs and for cr-POE and full-IPNs, respectively. The semi-IPNs, except for S-17 and S-66, exhibit sharp single peaks in both E'' and tan δ curves. The POE-rich S-17 specimen shows a broad transition region with the peak at a temperature slightly below the POE melting region. The PAA-rich S-66 specimen exhibits two peaks in the E'' curve: One at the peak for the equimolar S-50 specimen and another at the T_g for PAA, corresponding to the large shoulder and peak, respectively, in the tan δ curve. The full-IPNs, except for F-15 also, exhibit sharp single peaks similar to those for the semi-IPNs. The F-15 specimen has a peak similar to but not as broad as that for the S-17 specimen. The F-65 specimen, differing from the S-66 specimen, shows only one peak with a small shoulder. The loss maximum temperature T_{max} of the semi-IPNs shows a composition dependence similar to that of the brittle point T_b for POE : PAA blends reported by Smith *et al.*[13] as shown in Figure 2. On the other hand, the T_{max} of the full-IPNs shows a composition dependence similar to that of the T_g of the IPNs determined by DSC. Thus, even in POE rich

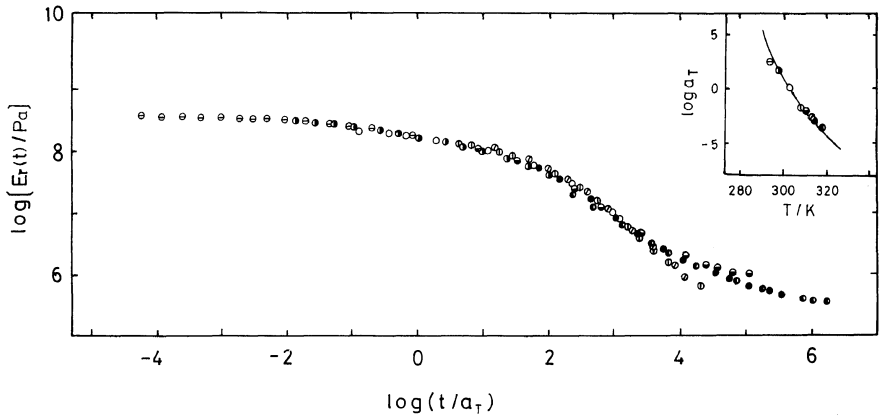

Figure 5. The stress relaxation master curve for S-50 with the reference temperature $T_r = 303$ K. The insert shows a plot of the shift factor $\log a_T$ *versus* T.

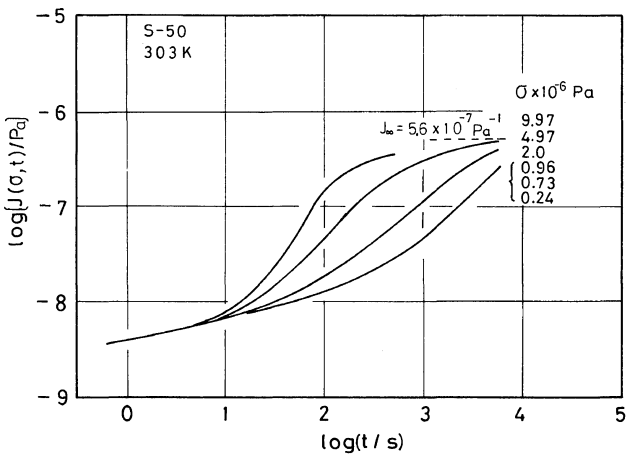

Figure 6. Plots of stress dependent creep compliance $J(\sigma, t)$ *versus* $\log t$ for S-50 at 303 K with the stress σ as indicated.

samples, the degree of crystallinity χ_c of the POE phase is very small, and the samples behave as single-phase material.

These results suggest that each of the semi- and full-IPNs with a PAA content between 30 and 60 mol% has a single phase in which either amorphous POE or PAA is mixed with the POE : PAA complex. The IPNs with low PAA content have microphase-separated POE domains and the POE : PAA complex domains, while those with high PAA content have PAA domains and the complex domains. Apparently, as seen from the dynamic mechanical data, the extent of microphase separation is far less significant in the full-IPNs than in the semi-IPNs. The preexisting crosslinks in the POE domains may hamper the occurrence of microphase separation.

Stress Relaxation and Creep Behavior

Figure 5 shows the tensile stress relaxation master curve for the equimolar semi-IPN S-50 with the reference temperature $T_r = 303$ K. The superimposition of the data is fairly satisfactory except for those at longer times. This implies that the complex dissociation occurs only at longer times under small strains. Plots of log (shift factor a_T) *versus* temperature are shown in the insert of Figure 5, where the solid curve represents the WLF equation.[18]

Figure 6 shows the nonlinear creep compliance $J(\sigma, t)$ obtained at 303 K for the S-50 specimen. It can be seen that $J(\sigma, t)$ is approximately independent of the stress σ below 1.0 MPa. Beyond this value of σ, $J(\sigma, t)$ deviates from the linear relation and exhibits a distinct sigmoidal shape. With increasing σ, the curve approaches more rapidly the asymptote of $J_\infty/\mathrm{MPa} = 0.56$, as in the case of PEA/PMMA IPNs.[8]

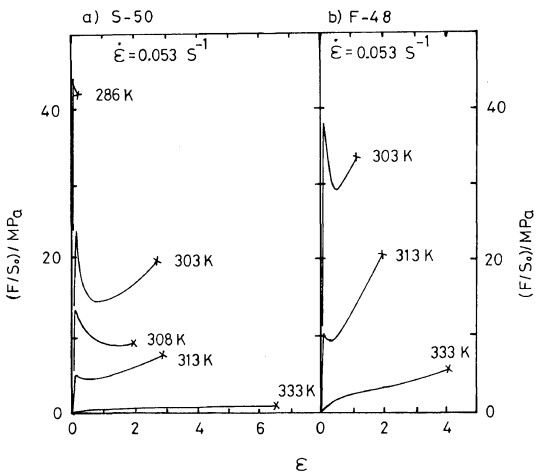

Figure 7. Stress-strain curves for (a) S-50 and (b) F-48 with $\dot{\varepsilon} = 0.053\,\mathrm{s}^{-1}$ at various temperatures as indicated. Marks (×) denote break points.

Stress-Strain Curves

Figure 7 shows the stress-strain curves for (a) S-50 and (b) F-48 obtained with $\dot{\varepsilon} = 0.053\,\mathrm{s}^{-1}$ at various temperatures as indicated. The curves for both specimens change from soft-and-weak rubbery behavior to hard plastic-like behavior as the tem-

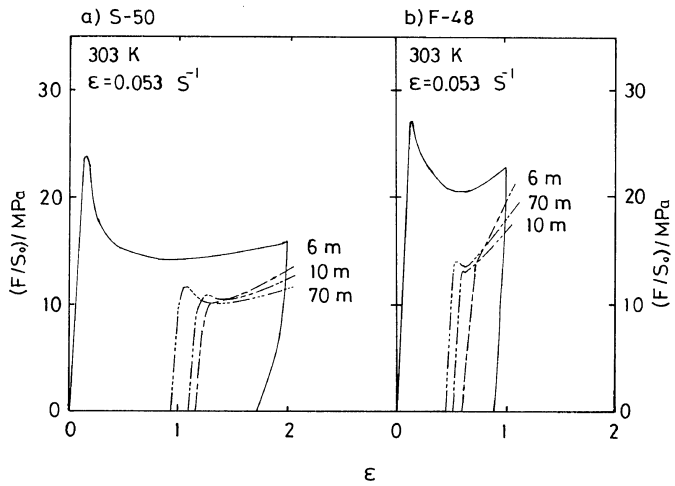

Figure 8. Stress-strain hysteresis curves for (a) S-50 and (b) F-48 at 303 K after certain rest times as indicated. Solid curves represents the first run.

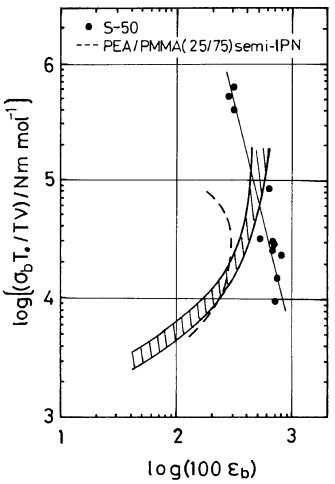

Figure 9. Failure envelope, *i.e.*, plots of $\log(T_0\sigma_b/\nu T)$ *versus* $\log \varepsilon_b$ for S-50 with $T_0 = 333$ K obtained from the tensile rupture behavior. Broken curve represents that for semi-IPNs with 75 wt% PMMA content.[8] Shaded area indicates the region where most of the homopolymer–elastomer data fall.[19]

perature decreases from 333 to 286 K. However, compared to the curves of S-50, these of the F-48 specimen exhibit a higher yield strength and a sharper upturn as a result of the stretching of the POE network and the higher modulus. The cause for these differences can be ascribed to the preexisting crosslinks in the POE domains. Even at low temperatures where a distinct yield point was apparent in the stress-strain curve, the S-50 specimen could be elongated uniformly until breaking and showed no necking. Also, no stress-whitening was observed. On the other hand, the F-48 specimen showed necking, and resumed its original length when annealed at 333 K for 4 h. The yielding phenomena may be associated with the complex dissociation by stretching.

Figure 8 shows the stress-strain hysteresis curves at 303 K for (a) S-50 and (b) F-48 specimens stretched 300% and 200% elongation, respectively. The first run for either specimen exhibited a clear yield point. When the tension was released, the specimens underwent hardly any shrinkage. After resting for six min each specimen shrank to about half its length and in the second run, there was no yield point. The second runs following rest periods of 10 minutes and 70 minutes showed yield points but the specimens did not recover their original length on releasing the stress. During the rest period, the complex could be partly reformed between the POE and PAA segments in the elongated state.

The effects of complex dissociation and reformation can be seen in the reduced failure envelope. Figure 9 shows the plots of $\log(T_0\sigma_b/\nu T)$ *versus* $\log \varepsilon_b$ for the S-50 specimen. Here, the reference temperature T_0 was chosen as 333 K, and the σ_b and ε_b are the ultimate stress and strain at break, respectively, and ν is the effective network chain density. For comparison, the envelope for PEA/

PMMA semi-IPN[8] is also shown in the figure. The POE : PAA IPN S-50 exhibited an envelope distinctly different from those of PEA/PMMA IPNs. During the stretching at low strain rates, the complex dissociation and reformation may possibly take place repeatedly, allowing the specimen to reach a high extension ratio with a small stress. On the other hand, during the stretching at high strain rates, complex dissociation and reformation hardly occur before the specimen breaks. Therefore, σ_b is much larger, while ε_b is smaller than those at low strain rates.

Acknowledgements. This work was supported in part by the Ministry of Education, Science and Culture (Mombusho) under Grants 147087 and 543026, which are gratefully acknowledged.

REFERENCES AND NOTES

1. To distinguish various topologically different species of polymer alloys (=multicomponent polymers) made from the same constituent polymers, poly(A) and poly(B), we employ the following conventions: Block and graft copolymers are designated as PA-PB; polymer blends and interpenetrating polymer networks (IPNs) as PA/PB, in which the presence of covalent bonds between the two components is unimportant; and polymer complexes or complex-forming systems as PA:PB, in which secondary interactions prevail.
2. "Polymer Alloys," (in Japanese), T. Kotaka, F. Ide, T. Nishi, and K. Ogino, Ed., *Tokyo Kagakudojin*, Tokyo, 1981.
3. A. A. Donatelli, D. A. Thomas, and L. H. Sperling, "Recent Advances in Polymer Blends, Grafts and Blocks," L. H. Sperling, Ed., Plenum Press, New York, 1974.
4. H. L. Frisch, K. C. Frisch, and D. Klempner, "Chemistry and Properties of Crosslinked Polymers," S. S. Labana, Ed., Academic Press, New York, 1976, p 205.
5. J. A. Manson and L. H. Sperling, "Polymer Blends and Composites," Plenum Press, New York, 1976.
6. L. H. Sperling, *J. Polym. Sci., Macromol. Rev.*, **12**, 141 (1977).
7. H. Adachi and T. Kotaka, *Rep. Progr. Polym. Phys. Jpn.*, **23**, 371 (1980).
8. H. Adachi and T. Kotaka, *Polym. J.*, **14**, 379 (1982).
9. E. Tsuchida and Y. Osada, *Kobunshi*, **22**, 384 (1973).
10. E. A. Bekturov and L. A. Bimendiana, "Advance in Polymer Science," Vol. 41, Springer-Verlag, Berlin, 1981, p 99.
11. A. S. Michaelis, *Ind. Eng. Chem.*, **57**, 32 (1965); A. S. Michaelis and H. J. Bixler, "Encycl. Chem. Technol.," Vol. 10, 2nd ed, Intersciences, New York, 1968, p 117; H. J. Bixler and A. S. Michaelis, "Encycl. Polym. Sci. Technol.," Vol. 10, H. F. Mark, N. M. Bikales, Ed., Interscience, New York, 1969, p 765.
12. E. Tsuchida, Y. Osada, and H. Ohno, *J. Macromol. Sci., Phys.*, **B17**, 683 (1980); E. Tsuchida and Y. Osada, *J. Polym. Sci., Polym. Chem. Ed.*, **13**, 559 (1975).
13. K. L. Smith, A. E. Winslow, and D. E. Petersen, *Ind. Eng. Chem.*, **51**, 1361 (1959).
14. Y. Mori and H. Tanzawa, *J. Appl. Polym. Sci.*, **20**, 1775 (1976).
15. Y. Osada and Y. Takeuchi, *J. Polym. Sci., Polym. Lett. Ed.*, **19**, 303 (1981).
16. S. Nishi, H. Adachi, and T. Kotaka, *Rep. Progr. Polym. Phys. Jpn.*, **24**, 5 (1981); S. Nishi, H. Adachi, and T. Kotaka, *ibid.*, **24**, 299 (1981).
17. C. S. Fuller, *Chem. Revs.*, **26**, 143 (1940).
18. J. D. Ferry, "Viscoelastic Properties of Polymers," 3rd ed, John Wiley, New York, 1980.
19. R. F. Landel and R. F. Fedors, "Deformation and Fracture of High Polymer," H. K. Kausch, J. A. Hassel, and R. I. Joffee, Ed., Plenum Press, New York, 1972, p 131.